Rhenium complexes of chromophore-appended dipicolylamine ligands: syntheses, spectroscopic properties, DNA binding and X-ray crystal structure†

Lucy A. Mullice,[a] Rebecca H. Laye,[b] Lindsay P. Harding,[c] Niklaas J. Buurma*[a] and Simon J. A. Pope*[a]

Received (in Durham, UK) 22nd January 2008, Accepted 17th June 2008
First published as an Advance Article on the web 22nd August 2008
DOI: 10.1039/b800999f

The syntheses of two chromophore-appended dipicolylamine-derived ligands and their reactivity with pentacarbonylchlororhenium have been studied. The resultant complexes each possess the *fac*-$Re(CO)_3$ core. The ligands $\mathbf{L^1}$ 1-[bis(pyridine-2-ylmethyl)amino]methylpyrene and $\mathbf{L^2}$ 2-[bis(pyridine-2-ylmethyl)amino]methylquinoxaline were isolated *via* a one-pot reductive amination in moderate yield. The corresponding rhenium complexes were isolated in good yields and characterised by ^{1}H NMR, MS, IR and UV-Vis studies. X-Ray crystallographic data were obtained for *fac*-$\{Re(CO)_3(\mathbf{L^1})\}(BF_4)$, $C_{34}H_{26}BF_4N_4O_3Re$: monoclinic, $P2(1)/c$, a = 18.327(2) Å, α = 90.00°, b = 14.1537(14) Å, β = 96.263(6)°, c = 23.511(3) Å, γ = 90.00°, 6062.4(11) Å^3, Z = 8. The luminescence properties of the ligands and complexes were also investigated, with the emission attributed to the appended chromophore in each case. Isothermal titration calorimetry suggests that *fac*-$\{Re(CO)_3(\mathbf{L^1})\}(BF_4)$ self-aggregates cooperatively in aqueous solution, probably forming micelle-like aggregates with a cmc of 0.18 mM. Investigations into the DNA-binding properties of *fac*-$\{Re(CO)_3(\mathbf{L^1})\}(BF_4)$ were undertaken and revealed that *fac*-$\{Re(CO)_3(\mathbf{L^1})\}(BF_4)$ binding to fish sperm DNA (binding constant 1.5 ± 0.2 × 10^5 M^{-1}, binding site size 3.2 ± 0.3 base pairs) is accompanied by changes in the UV-Vis spectrum as typically observed for pyrene-based intercalators while the calorimetrically determined binding enthalpy (−14 ± 2 kcal mol^{-1}) also agrees favourably with values as typically found for intercalators.

Introduction

The continued development of the coordination chemistry of Re^I, principally in its *fac*-$\{Re(CO)_3\}$ guise, is driven by a variety of applications. Firstly, not only is Re an excellent chemical analogue for the radioisotope ^{99m}Tc ($t_{\frac{1}{2}}$ = 6.01 h, γ = 142.7 keV) which is routinely used in single photon emission-computed tomography, but radioisotopes of Re itself such as $^{186/188}$Re (^{186}Re $t_{\frac{1}{2}}$ = 3.68 days, β = 1.07 MeV, γ = 137 keV; ^{188}Re $t_{\frac{1}{2}}$ = 16.98 h, β = 2.12 MeV, γ = 155 keV) may well be utilised in the future with regard to radiopharmaceutical therapy.[1,2] A fundamental breakthrough within this area was achieved by Alberto and co-workers who developed the chemistry of *fac*-$\{M(CO)_3(H_2O)_3\}^+$ (M = Tc): a crucial step in the development of functionalised therapeutics for nuclear medicine.[3] Additional interest in Re^I coordination chemistry has been motivated by the photophysical properties of diimine complexes which are usually luminescent in the visible region as a consequence of a metal-to-ligand charge transfer (MLCT) excited state.[4,5] This emission can often be long-lived (up to a microsecond) and with good quantum yields (especially in comparison with emissive diimine complexes of Ru^{II} or Os^{II}). These emissive attributes are coupled with favourable long-wave excitation (the MLCT absorption is often into the visible region) which should eventually lead to such compounds being further exploited for biological microscopy applications.[6] The likelihood of such an eventuality is further enhanced when considering the relative ease of syntheses for water soluble and water stable derivatives.

In this study we were interested in investigating the Re^I coordination chemistry of some chromophore-appended dipicolyl amine ligands (Fig. 1). The chromophores of choice

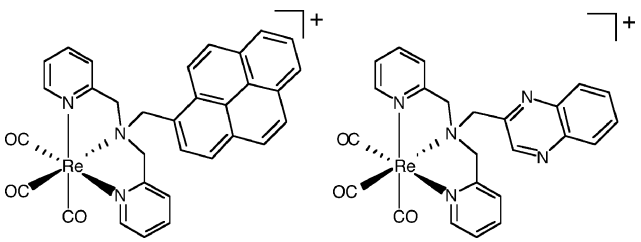

Fig. 1 Cationic chromophore-appended complexes isolated in this study.

[a] *School of Chemistry, Cardiff University, Park Place, Cardiff, Cymru/WalesUK CF10 3AT. E-mail: buurma@cardiff.ac.uk. E-mail: popesj@cardiff.ac.uk; Fax: +44 2920874030; Tel: +44 2920879316*
[b] *Department of Chemistry, The University of Sheffield, Dainton Building, Brook Hill, Sheffield, UK S3 7HF*
[c] *School of Biological and Chemical Sciences, University of Huddersfield, Queen Street, Huddersfield, UK HD1 3DH*

† Electronic supplementary information (ESI) available: Electrospray mass spectra of *fac*-$\{Re(CO)_3(L^n)\}(BF_4)$, a lifetime decay profile for $\mathbf{L^1}$, and CD titration for *fac*-$\{Re(CO)_3(L^n)\}(BF_4)$. CCDC reference number 688593. For ESI and crystallographic data in CIF format see DOI: 10.1039/b800999f

in this study were pyrene and quinoxaline moieties. As well as allowing longer wavelength sensitisation (potentially up to 400 nm), pyrene containing molecules often possess useful UV-visible luminescent characteristics based on both monomer (380–420 nm) and excimer (450–500 nm) emission. Consequently, pyrene derivatives have been used in many wide ranging applications such as in sensors (for alkali metals,[7] sugars,[8] electron deficient molecules,[9] pyrophosphate,[10] Hg^{II} [11], Zn^{II} [12]), in molecular logic circuits,[13] Fe^{III}-driven switches,[14] ion pair recognition,[15] oligodeoxynucleotide probes for the detection of base insertion[16] and more conventionally as chromophoric antennae for both d-metal[17] and lanthanide-based assemblies.[18] Indeed chromophore-appended Re^{I} complexes have recently been utilised for cell microscopy.[19] In addition to its use as a chromophore, pyrene is a known DNA-intercalator and can be used to drive interactions with DNA.[20–23] DNA-anchoring of metal centres is useful for biocompatibilisation. In addition, the association of catalytic metal centres with DNA has successfully been used in the generation of hybrid catalysts resulting in highly enantioselective catalytic reactions.[24]

In this paper we discuss the synthesis of chromophore-appended tripodal ligands and their Re^{I} complexes as well as some preliminary findings with regard to DNA binding studies of the pyrenyl example.

Results and discussion

Syntheses

The ligands $\mathbf{L^1}$ [25] and $\mathbf{L^2}$ were synthesised according to a reductive amination coupling using a monohydride source as reducing agent (Scheme 1). Despite the steric bulk of the aldehydic groups, this synthetic approach was reasonably rapid and moderately yielding. Each ligand was purified using column chromatography (silica), with initial elution with CH_2Cl_2 removing unreacted aromatic aldehyde; the major fluorescent band was obtained eluting with 5% CH_3OH in CH_2Cl_2. In the case of $\mathbf{L^1}$ the product was obtained as a yellow oil which solidified over time to give a pale yellow crystalline solid. In contrast, $\mathbf{L^2}$ was obtained as a brown oil. Reaction of the free ligands with chloropentacarbonylrhenium in toluene at 100 °C gave the intermediate, bidentate complexes *fac*-{$ReCl(CO)_3(L^n)$} (where $n = 1, 2$) which precipitated from solution as the reaction progressed. Chloride abstraction with $AgBF_4$ in MeCN at 60 °C yielded the corresponding cationic, tridentate complexes, *fac*-{$Re(CO)_3(L^n)$}(BF_4) as pale off-white (for $\mathbf{L^1}$) or yellow ($\mathbf{L^2}$) powders (Scheme 2). Although the use of *fac*-$\{ReBr_3(CO)_3\}^{2-}$ has been shown to allow easy access to complexes of the form *fac*-$\{Re(CO)_3(L)_3\}^{+}$, this precursor itself is also derived from bromopentacarbonylrhenium.[26]

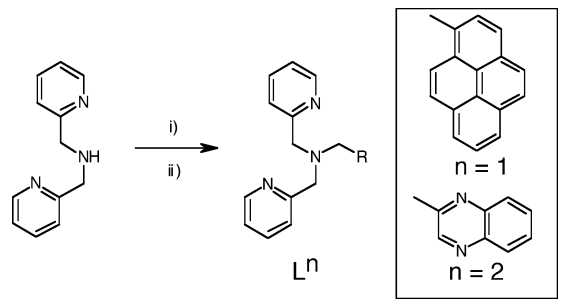

Scheme 1 Syntheses of the ligands: (i) 1 eq. 2-pyrenecarboxaldehyde or 2-quinoxalinecarboxaldehyde, 1 eq. $NaBH(OAc)_3$; (ii) aq. $NaHCO_3$, EtOAc extraction.

Characterisation and spectroscopic properties

Both ligands $\mathbf{L^{1/2}}$ gave satisfactory ^1H and $^{13}C\{^1H\}$ NMR spectra. The dominant features in the electrospray mass spectra reveal the parent ion peaks at m/z 414 and 342 for $\mathbf{L^1}$ and $\mathbf{L^2}$, respectively, corresponding to the mono-protonated forms. The UV-Vis absorption spectra of the free ligands in acetonitrile are dominated by π–π* transitions associated with the pyridyl (260–280 nm), pyrene (340–300 nm) and quinoxaline (320–300 nm) units.

^1H NMR studies (Fig. 2), in $CDCl_3$, on *fac*-{$ReCl(CO)_3(\mathbf{L^1})$} allowed the specific binding mode of the ligand to be deduced. The aromatic portion of the spectrum showed that the two pyridyl units were equivalent and shifted downfield with respect to the free ligand, suggesting that both pyridyl units are coordinated to the rhenium centre. The methylene linker units also show significant deviations in chemical shift from the corresponding free ligand. The pyrenyl methylene linker was observed as a singlet at *ca.* 5.5 ppm. Two sets of resonances were assigned to the diastereotopic protons of the pyridyl methylene linkers; each integrate to two protons and each have a coupling constant of 17 Hz, confirming a geminal two-bond coupling. After chloride abstraction, the chemical shifts associated with these methylene linker groups changed significantly (Fig. 2), suggesting a modulation in coordination environment. Interestingly there is a slight upfield shift associated with the pyrene-bound methylene resonance. The minor alterations in the pyridyl resonances also confirm an alteration in coordination environment following halide abstraction.

The ^1H NMR spectra of the related quinoxaline derivatives were similar, suggesting the same sequence of coordination modes. However, for the intermediate complex of $\mathbf{L^2}$ we noted a lack of diastereotopicity associated with the pyridyl methylene linkers, instead observing a broadened resonance at ~5.2 ppm. The diastereotopicity returned upon treatment with $AgBF_4$ and presumably, a more rigid coordination conformation. Importantly the ^1H NMR spectra for the $\mathbf{L^2}$ complexes also suggest that the nitrogen heteroatoms of the quinoxaline moiety were not contributing to the coordination sphere of the rhenium ion. The signature C3-bound proton (shifted furthest downfield, singlet at 9.05 ppm in $\mathbf{L^2}$) of the quinoxaline unit would be expected to shift if the quinoxaline itself was coordinated.[27] In fact the ^1H NMR spectra of the corresponding

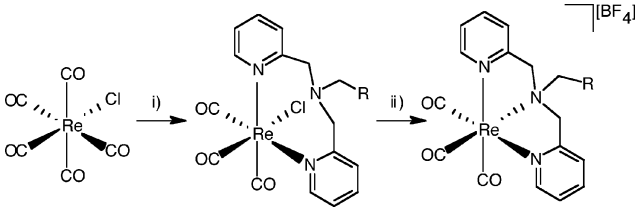

Scheme 2 Syntheses of the rhenium complexes: (i) 1 eq. L^n, toluene, 100 °C, 3 h; (ii) 1 eq. $AgBF_4$, MeCN, 60 °C, 24 h.

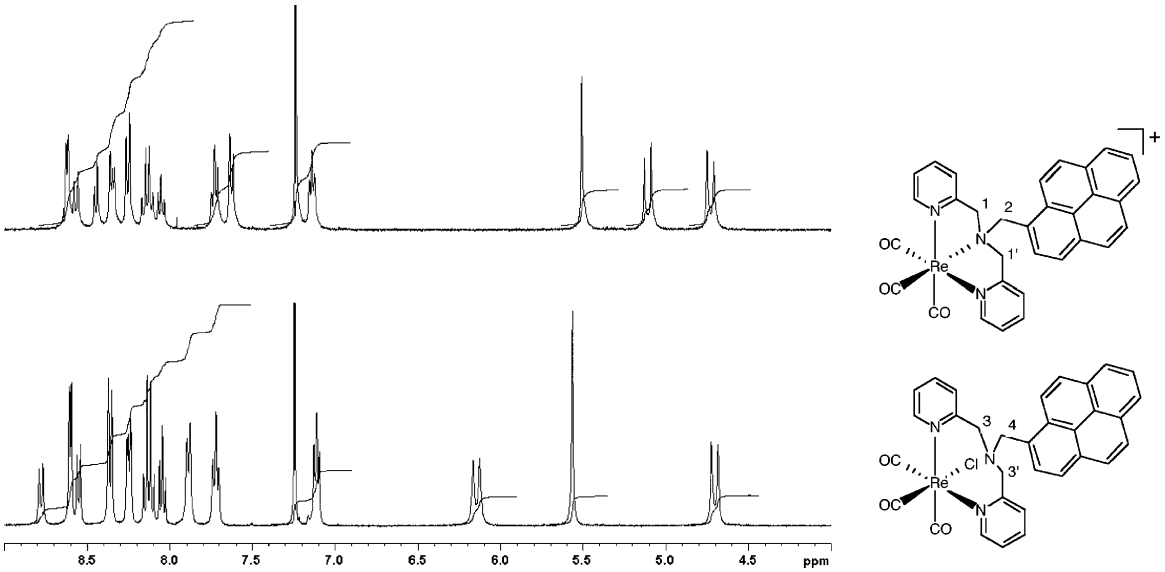

Fig. 2 ^{1}H NMR spectra of *fac*-{Re(CO)$_3$(**L^1**)}(BF$_4$) (top) and *fac*-{ReCl(CO)$_3$(**L^1**)} (bottom). Both spectra were recorded at room temperature in $CDCl_3$.

complexes, *fac*-{ReCl(CO)$_3$(**L^2**)} and *fac*-{Re(CO)$_3$(**L^2**)}(BF$_4$), revealed that this resonance remained at around 9.0 ppm.

Solution state (chloroform) IR studies were utilised to probe the rhenium-bound carbonyl groups. For the pyrene appended complex *fac*-{ReCl(CO)$_3$(**L^1**)} ν(CO) were observed at 2033, 1935 and 1916 cm^{-1} whilst the quinoxaline analogue gave 2032, 1934 and 1921 cm^{-1}. These three stretches are indicative of a *fac*-tricarbonyl arrangement of local C_s symmetry, again suggesting that both pyridyl units are bound as opposed to one pyridyl and the bridging amine. Surprisingly, the ν(CO) values for the chloride-abstracted cationic complexes do not show major changes from their neutral precursors. In the absence of the ^{1}H NMR data this would have suggested that the ligand is coordinated in a tridentate form and that the precipitation of AgCl from the reaction mixture was merely a consequence of counter anion exchange. Unfortunately mass spectrometry did not allow differentiation between the intermediate and final cationic complexes. The high resolution electrospray data (see ESI†) associated with the intermediate complexes, *fac*-{ReCl(CO)$_3$(L^n)}, showed a single cluster of peaks with the appropriate isotopic distribution for {M − Cl}$^+$. Ionisation-induced loss of the axial chloride ligand to form the cationic fragment is a common observation in the mass spectra of species of this type, but is often accompanied by addition of solvent (samples run in acetonitrile will often form the cationic MeCN adduct following ionisation). The results for the final cationic complexes corresponded to {M}$^+$ and as a consequence were indistinguishable from the results given by the intermediate species. Therefore in the absence of a single crystal X-ray structural investigation of the intermediate species *fac*-{ReCl(CO)$_3$(L^n)} the assigned coordination mode remains a tentative one.

Single crystal X-ray structural determination of *fac*-{Re(CO)$_3$(**L^1**)}(BF$_4$)

Colourless, block-like single crystals suitable for X-ray analysis were obtained *via* vapour diffusion of diethyl ether into a concentrated chloroform solution of the complex, over a 3 day period at room temperature. The study confirmed the integrity of the proposed ligand framework and the proposed coordination geometry of the complex with two unique whole molecules in the asymmetric cell together with two tetrafluoroborate counterions. The parameters associated with the crystal data are shown in Table 1, with selected bond lengths and bond angles reported in Table 2. As represented in Fig. 3 the structure of the molecular cation reveals the integrity of the *fac*-tricarbonyl rhenium unit together with the facially capping dipicolylamine-functionalised ligand in an N$_3$ coordinated mode. The pendant pyrene unit is positioned away from the rhenium core.

The Re–CO bond lengths are typical (1.918–1.930 Å) of those observed in related examples.[26] The relative

Table 1 Crystal data collection and refinement details for the crystal structure for *fac*-{Re(CO)$_3$(**L^1**)}(BF$_4$)[a]

Empirical formula	$C_{34}H_{26}BF_4N_4O_3Re$
Formula weight	811.60
Temperature	100(2) K
Wavelength	0.71073 Å
Crystal system	Monoclinic
Space group	*P*2(1)/*c*
Unit cell dimensions	*a* = 18.327(2) Å, *α* = 90.00°
	b = 14.1537(14) Å, *β* = 96.263(6)°
	c = 23.511(3) Å, *γ* = 90.00°
Volume	6062.4(11) Å^3
Z	8
Density (calculated)	1.778 Mg m^{-3}
Absorption coefficient	4.077 mm^{-1}
F(000)	3184
Crystal size	0.28 × 0.20 × 0.05 mm^3
θ range for data collection	1.68 to 33.55°
Reflections collected	23 593
Independent reflections	18 225
Refinement method	Full-matrix least squares on *F*
Goodness-of-fit on *F*	0.950
Final *R* indices [$I > 2\sigma(I)$]	*R*1 = 0.0285, w*R*2 = 0.0512
R indices (all data)	*R*1 = 0.0497, w*R*2 = 0.0572

[a] The structure was refined on F_o^2 using all data.

Table 2 Selected bond lengths and bond angles for *fac*-{Re(CO)$_3$($\mathbf{L^1}$)}(BF$_4$)

Bond lengths/Å			
Re(1)–C(30)	1.918(2)	Re(2)–C(62)	1.925(2)
Re(1)–C(31)	1.930(2)	Re(2)–C(63)	1.924(2)
Re(1)–C(32)	1.919(2)	Re(2)–C(64)	1.928(2)
Re(1)–N(1)	2.2246(18)	Re(2)–N(4)	2.2287(18)
Re(1)–N(2)	2.1729(18)	Re(2)–N(5)	2.1694(18)
Re(1)–N(3)	2.1749(18)	Re(2)–N(6)	2.1743(19)
N(1)–C(1)	1.503(3)	N(4)–C(33)	1.502(3)
N(1)–C(7)	1.502(3)	N(4)–C(39)	1.500(3)
N(1)–C(13)	1.519(3)	N(4)–C(45)	1.521(3)
Bond angles/°			
C(30)–Re(1)–C(31)	86.44(9)	C(62)–Re(2)–C(63)	89.25(10)
C(30)–Re(1)–C(32)	89.44(10)	C(62)–Re(2)–C(64)	88.75(10)
C(31)–Re(1)–C(32)	87.76(9)	C(63)–Re(2)–C(64)	89.75(10)
C(30)–Re(1)–N(1)	173.47(8)	C(62)–Re(2)–N(4)	172.79(8)
C(31)–Re(1)–N(1)	98.27(8)	C(63)–Re(2)–N(4)	95.49(8)
C(32)–Re(1)–N(1)	94.74(8)	C(64)–Re(2)–N(4)	96.68(8)
C(30)–Re(1)–N(2)	97.78(8)	C(62)–Re(2)–N(5)	95.24(8)
C(31)–Re(1)–N(2)	175.08(8)	C(63)–Re(2)–N(5)	95.43(8)
C(32)–Re(1)–N(2)	94.76(8)	C(64)–Re(2)–N(5)	173.49(9)
C(30)–Re(1)–N(3)	96.52(8)	C(62)–Re(2)–N(6)	97.53(9)
C(31)–Re(1)–N(3)	100.07(8)	C(63)–Re(2)–N(6)	171.77(8)
C(32)–Re(1)–N(3)	170.11(8)	C(64)–Re(2)–N(6)	95.04(9)
N(1)–Re(1)–N(2)	77.32(6)	N(4)–Re(2)–N(5)	78.94(7)
N(1)–Re(1)–N(3)	78.26(7)	N(4)–Re(2)–N(6)	77.34(7)
N(2)–Re(1)–N(3)	77.00(7)	N(5)–Re(2)–N(6)	79.37(7)

hybridisation of the nitrogen donors was confirmed by the Re–N distances, where Re–N(1) (sp^3) at 2.2246(18) Å is significantly longer than either Re–N(2) or Re–N(3) (sp^2), each *ca.* 2.173 Å. The coordination geometry at rhenium is not of an ideal octahedral arrangement. This deviation appears to be a result of the tridentate N$_3$-chelating unit and the formation of two five-membered rings at rhenium, which consequently results in N–Re–N angles $<80°$. Despite the presence of highly planar aromatic units the crystal packing of the molecule does not appear to be dominated by intermolecular π–π interactions (Fig. 3). The most notable observation is an intermolecular pyridine–pyrene distance of *ca.* 3.4 Å (Fig. 4).

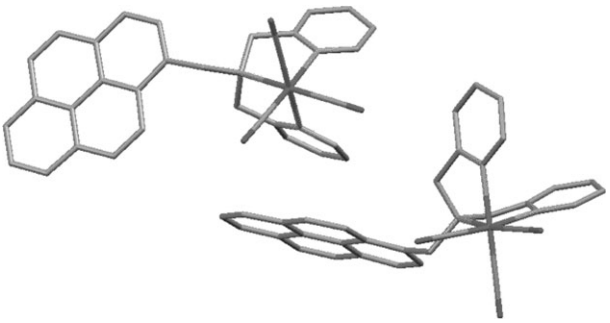

Fig. 4 Diagram showing the nearest intermolecular π–π interaction of *ca.* 3.4 Å, between a coordinated pyridyl and a neighbouring pyrene unit.

UV-Vis and preliminary luminescence studies

The absorption spectra of the complexes closely resemble those of the free ligands. For the complexes of $\mathbf{L^1}$ the spectra are dominated by ligand-based transitions $^1\pi\pi^*$ between 270 and 345 nm. The higher energy transitions are due to the pyridyl units whereas the lower energy transitions, for example at 345 nm, are pyrenyl in origin. This is in contrast to bis-imine complexes of Re^I which tend to be brightly coloured due to the presence of a MLCT transition around 360–420 nm.[4] For the quinoxaline-derived species of $\mathbf{L^2}$ the observations are similar: electronic spectra appear to be dominated by ligand-centred transitions between 260 and 320 nm. Thus, on the basis of these results, for each Re^I complex the lowest energy absorption can be predominantly attributed to ligand-centred transitions of the appended chromophore.

Photophysical studies were undertaken in aerated acetonitrile. In the case of $\mathbf{L^1}$ an excitation wavelength of 340 nm, at which pyrene absorption dominates, was utilised with a sample concentration of $<10^{-5}$ M. The steady state emission spectrum of the free ligand generated characteristic vibronically structured pyrene-based emission between 300–400 nm, assigned to fluorescence from the $^1\pi\pi^*$ (S$_1$) state. Despite the hydrophobicity of $\mathbf{L^1}$ very little excimer emission was observed *ca.* 480 nm at this concentration. Following irradiation at 320 nm $\mathbf{L^2}$ revealed a far less structured, broad emission band at around 400 nm, consistent with quinoxaline-localised fluorescence.

The rhenium complexes displayed emission properties that can be attributed to the appended chromophores. This is reasonable since although quinoline-derived analogues of

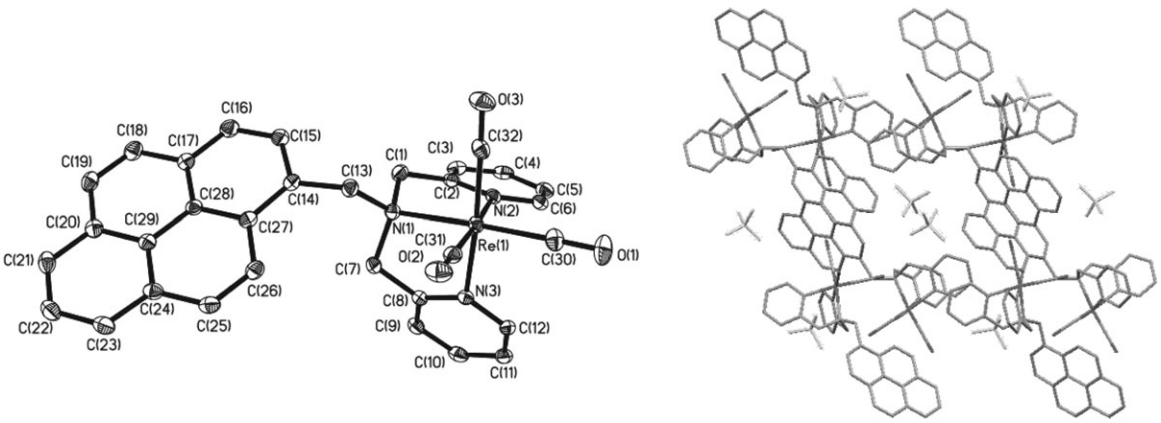

Fig. 3 Left: structural representation of *fac*-{Re(CO)$_3$($\mathbf{L^1}$)}(BF$_4$) with 50% probability ellipsoids (counterion omitted for clarity). Right: packing diagram (counterion included) viewed along the *c* axis.

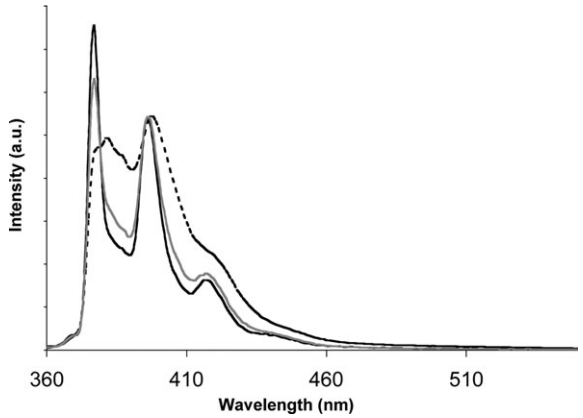

Fig. 5 Steady state emission spectra of the pyrene-containing species following excitation at 340 nm. $\mathbf{L^1}$ (--), *fac*-{$ReCl(CO)_3(\mathbf{L^1})$} (—) and *fac*-{$Re(CO)_3(\mathbf{L^1})$}{BF_4} (grey). All spectra were obtained in aerated acetonitrile and are normalised at 397 nm.

DPA-type ligands are known to display visible MLCT (Re $d\pi \rightarrow$ quinoline π^*) emission,[26] Dipicolyl amine (DPA) systems generally do not. Fig. 5 compares the fluorescence spectra of the pyrene-containing species $\mathbf{L^1}$, *fac*-{$ReCl(CO)_3(\mathbf{L^1})$} and *fac*-{$Re(CO)_3(\mathbf{L^1})$}{BF_4}. The principal differences between the spectra of the complexes are the relative intensities of the vibrational bands.

Time-resolved lifetime measurements were undertaken on $\mathbf{L^1}$ and its complexes, focusing on the decay of the pyrene-centred $^1\pi\pi^*$ emission. Thus, with excitation and detection wavelengths of 355 nm and 395 nm, respectively, the lifetime of the pyrene-centred emission was obtained in aerated acetonitrile. For $\mathbf{L^1}$ the decay profile fitted best to a biexponential with corresponding lifetimes of $\tau = <1$ and 119 ns, with the longer component dominating (77%) (see ESI†). Multi-component decay is not unusual for pyrenyl containing species and is often attributed to the presence of conformers. In contrast, the fluorescence lifetimes obtained on the complexes *fac*-{$ReCl(CO)_3(\mathbf{L^1})$} and *fac*-{$Re(CO)_3(\mathbf{L^1})$}{BF_4} were dramatically shortened, in both cases reduced to <1 ns. Recent work into the fluorescence properties of functionalised pyrenes has asserted that the most important radiationless decay process is the depopulation of the S_1 state *via* inter-system crossing (ISC) yielding the triplet state.[28] We therefore propose that the reduction in pyrene fluorescence lifetime in *fac*-{$ReCl(CO)_3(\mathbf{L^1})$} and *fac*-{$Re(CO)_3(\mathbf{L^1})$}{BF_4} is due to rhenium-assisted ISC. Unfortunately de-aerated solutions of the complexes did not allow the spectroscopic detection of the triplet state and in the absence of a quantum yield for T_1 our assignment remains tentative. The quinoxaline-derived complexes both showed emission spectra dominated by the quinoxaline chromophore (Fig. 6) and characterised by a broad structureless fluorescence centred *ca.* 420 nm.

DNA-binding studies with *fac*-{$Re(CO)_3(\mathbf{L^1})$}{BF_4} ($\mathbf{ReL^1}$)

Self-aggregation. Isothermal titration calorimetry (ITC) shows a non-constant heat of dilution for $\mathbf{ReL^1}$ in a DMSO containing (10 vol%) buffer (Fig. 7). The sigmoidal dependence of the heat of dilution on the sample concentration in the calorimeter cell indicates that $\mathbf{ReL^1}$ self-aggregates

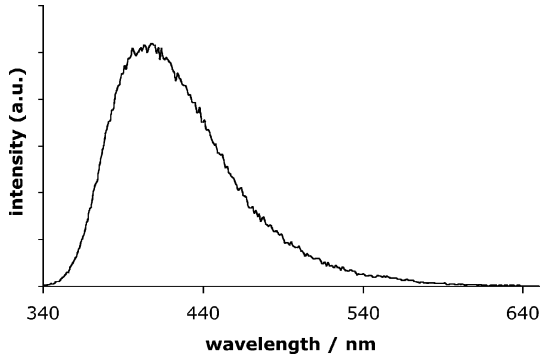

Fig. 6 Steady state emission spectrum for *fac*-{$Re(CO)_3(\mathbf{L^2})$}{BF_4} in aerated acetonitrile following excitation at 320 nm.

cooperatively, probably forming micelle-like aggregates. Fig. 7 shows that deaggregation upon dilution results in a type A enthalpogram[29] with a critical micelle concentration (cmc) of 0.18 mM and an enthalpy of micellisation ($\Delta_{mic}H$) of -5.8 kcal mol^{-1}. The strong tendency of pyrene to aggregate in aqueous solution results in the low cmc. The cationic *fac*-$Re(CO)_3$ core acts as a surfactant headgroup. The (ideal) type A enthalpogram is typical for surfactants displaying a low cmc, but the presence of DMSO is undoubtedly a contributing factor as well as DMSO disrupts pairwise solute–solute interactions which could otherwise have complicated the dilution enthalpogram.[29] Finally, the $\Delta_{mic}H$ of -5.8 kcal mol^{-1} is similar to the additional contribution of a pyrenyl group to the enthalpy of micellisation of pyrene-containing gemini surfactants.[30]

DNA binding. UV-Vis titrations involving $\mathbf{ReL^1}$ concentrations of 5 and 13 μM in the presence of varying concentrations of fish sperm DNA (Fig. 8) show a characteristic red-shift of the pyrene absorption spectrum, in line with previous observations for pyrene-based compounds intercalating between the base pairs of double-stranded DNA[20–23,31] and a negative induced CD (see ESI†). Fig. 8 further shows the absence of

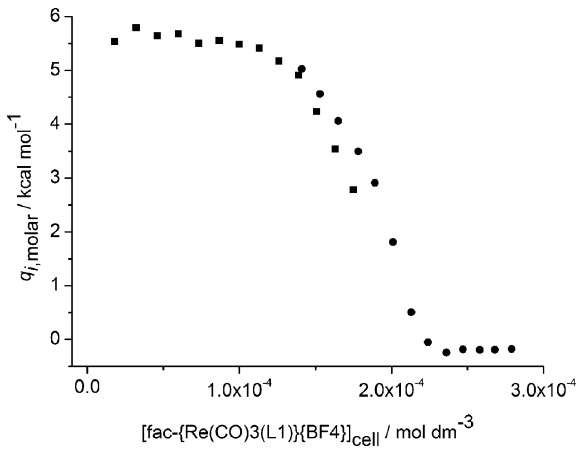

Fig. 7 Example of the molar heats of dilution of 1.0 mM *fac*-{$Re(CO)_3(\mathbf{L^1})$}{BF_4} in 22.5 mM MOPS titrated to pH 7.0, 0.9 mM EDTA, and 45 mM NaCl containing 10 vol% DMSO at 25 °C (composite titration resulting from 2 partial titrations—see experimental for details).

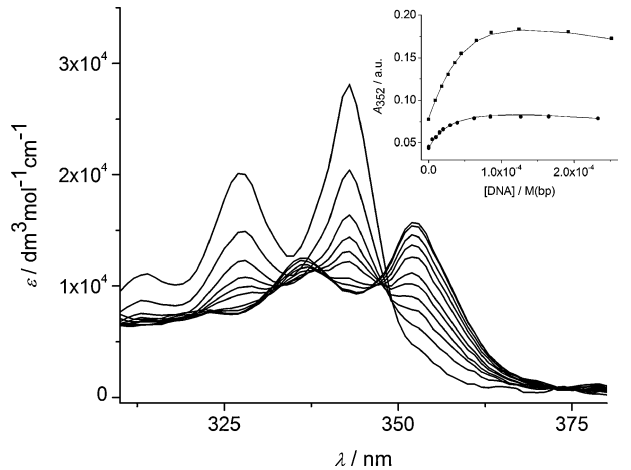

Fig. 8 UV-Vis titration involving sequential additions of fish sperm DNA to 13 μM *fac*-{$Re(CO)_3(\mathbf{L^1})$}(BF_4) in 25 mM MOPS titrated to pH 7.0, 1.0 mM EDTA, and 50 mM NaCl at 25 °C. Inset: absorbances at 352 nm (A_{352}) for titrations involving 5 μM (●) and 13 μM (■) *fac*-{$Re(CO)_3(\mathbf{L^1})$}(BF_4) analysed simultaneously in terms of a multiple-independent-site binding model.

tight isosbestic points, suggesting that the binding process involves more than a simple two-state binding process, though a near-isosbestic point is found at 348 nm. This, again, is in line with previous studies which indicate different binding affinities and different UV-Vis absorption spectra for pyrene derivatives binding in different intercalation sites, with binding to AT-rich regions being favoured.[20,22,23] For fish sperm DNA, the ten unique dinucleotide steps in principle result in ten different intercalation environments and **ReL^1** binding affinities for each of these intercalation binding sites could vary. Such variation in affinities for different dinucleotide steps has been demonstrated for other intercalators, *e.g.* daunomycin.[31] In addition, non-intercalative binding (*vide infra*) and **ReL^1** self-aggregation (*vide supra*) add further complexity to the observed equilibria.

The presence of this variety of binding sites with different binding affinities results in "internal competition" in typical spectroscopic titrations where DNA is added to a **ReL^1** solution. At low DNA/**ReL^1** ratios, the **ReL^1** binds to all available binding sites. At higher DNA/**ReL^1** ratios, the **ReL^1** preferably binds to higher affinity or specific sites as they become more available. In order to bind to these higher affinity sites, the **ReL^1** has to dissociate from one of the lower affinity binding sites.[32a] Of particular note in this respect is the appearance of the peak at 336 nm at higher DNA/**ReL^1** ratios. This peak at 336 nm is commonly observed for interactions of pyrene derivatives with AT-rich DNA, but not for interactions with poly dG·poly dC and poly$(dCdG)_2$. The appearance of the peak at 336 nm at higher DNA/**ReL^1** ratios therefore suggests some specificity of **ReL^1** for AT-rich DNA.

Despite this complexity, we analysed the binding data in order to obtain an indication of the DNA-binding affinity of **ReL^1** and for comparison with similarly determined literature binding affinities (Fig. 8, inset). Absorbance values for different combinations of concentrations of **ReL^1** and DNA at 352 nm (A_{352}) were extracted from the full spectra and analysed in terms of a simple multiple-independent-site binding model. The binding constant of $(1.5 \pm 0.2) \times 10^5\ M^{-1}$, with a corresponding binding site size of 3.2 ± 0.3 base pairs, is typical for cationic pyrene-derivatives.[21–23]

Further information on the binding modes of **ReL^1** with fish sperm DNA was obtained from ITC. Titrating **ReL^1** into a solution containing fish sperm DNA results in an enthalpogram (Fig. 9) displaying (at least) two distinct exothermic DNA-binding events followed by typical sample dilution heat effects (*cf.* Fig. 7). The stoichiometry for the first binding mode can in principle be estimated from the first inflection point in the enthalpogram for simple binding systems. For the present system involving various binding sites with different binding affinities, this is not strictly the case. Nevertheless, the estimated half-way point of the first set of binding events of 0.3 **ReL^1** per base pair resembles the binding site size of 3.2 ± 0.3 base pairs for **ReL^1** as observed in the UV-Vis titrations. The high stoichiometry found for the second binding event suggests that this binding mode involves non-specific electrostatic binding, a DNA-binding mode of cationically substituted pyrenes which was also suggested by others.[23] Similar behaviour has been observed for other cationic DNA-binders as well.[32] Non-specific electrostatic binding is accompanied by

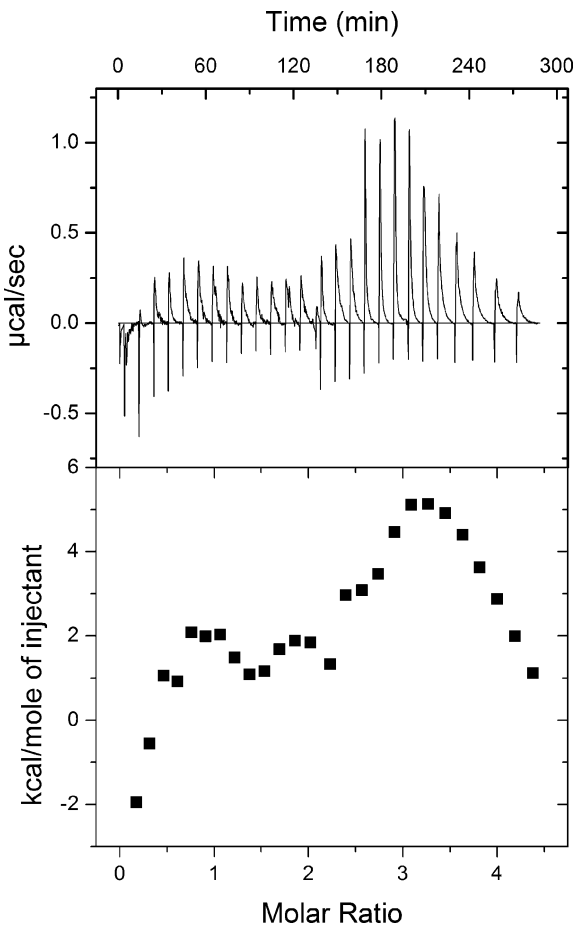

Fig. 9 Enthalpogram showing the molar heat effects of sequential additions of 1.0 mM *fac*-{$Re(CO)_3(\mathbf{L^1})$}(BF_4) to 100 μM fish sperm DNA in buffer (22.5 mM MOPS titrated to pH 7.0, 0.9 mM EDTA, and 45 mM NaCl containing 10 vol% DMSO) at 25 °C.

charge neutralisation. Visual inspection of the sample following ITC experiments shows that this charge neutralisation eventually results in precipitation of the DNA–**ReL^1** complex.

Finally, in order to obtain the interaction enthalpy for **ReL^1** intercalating between the base pairs of fish sperm DNA, the model free ITC approach[33] was used, giving an enthalpy change of -14 ± 2 kcal mol^{-1} (Fig. 10), in agreement with typical values found for intercalators.[34]

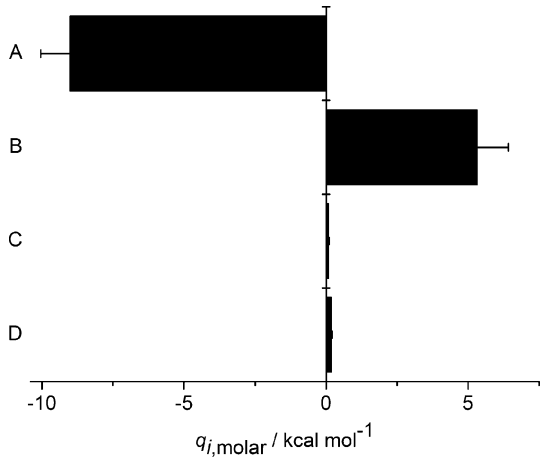

Fig. 10 (A) Averaged molar heat effect (error bars are standard deviations) for the titration of 1.0 mM *fac*-{Re(CO)$_3$(**L^1**)}(BF$_4$) into a 2.0 mM fish sperm DNA solution in buffer (22.5 mM MOPS titrated to pH 7.0, 0.9 mM EDTA, and 45 mM NaCl containing 10 vol% DMSO) at 25 °C up to a molar ratio (*fac*-{Re(CO)$_3$(**L^1**)}(BF$_4$): fish sperm DNA) of 0.05 and reference titrations: (B) *fac*-{Re(CO)$_3$(**L^1**)}(BF$_4$) into buffer, (C) buffer into fish sperm DNA, (D) buffer into buffer.

Conclusions

In this study we investigated the synthesis and photophysical properties of two chromophore-appended dipicolylamine ligands. Despite the relative bulk of the chromophores the ligands were accessible *via* a reductive amination procedure and the corresponding cationic *fac*-tricarbonyl Re^I complexes obtained through a two-step complexation process. The luminescent properties of the complexes were dominated by the appended organic chromophoric entity. Preliminary binding studies with fish sperm DNA, utilising the cationic pyrene-functionalised complex, suggest that binding to DNA is accompanied by changes in the UV-Vis spectrum as typically observed for pyrene-based intercalators with a binding constant of $1.5 \pm 0.2 \times 10^5$ M^{-1} and a binding site size of 3.2 ± 0.3 base pairs. The calorimetrically determined binding enthalpy also agrees favourably with values as typically found for intercalators. Titration calorimetry further suggests the presence of an electrostatically driven non-specific binding mode. These results suggest that the close proximity of the cationic metal centre does not inhibit the binding ability of the pyrene unit and therefore has implications for the biological application of such complexes in fluorescence microscopy or DNA–metal hybrid catalysts.

Experimental

General physical measurements

All photophysical data were obtained on a JobinYvon-Horiba Fluorolog spectrometer fitted with a JY TBX picosecond photodetection module and a Hamamatsu R5509-73 detector (cooled to −80 °C using a C9940 housing). The pulsed laser source was a Continuum Minilite Nd:YAG configured for 355 nm output. Lifetimes were obtained using the JY-Horiba FluorHub single photon counting module. IR spectra were recorded on a Varian 7000 FT-IR. Mass spectra were obtained using a Bruker MicroTOF LC. UV-Vis spectra were recorded using a Jasco 630 UV-visible spectrophotometer equipped with a Peltier temperature controller. The pH values of aqueous solutions were determined using a Hanna Instruments pH210 microprocessor pH meter with a VWR simple junction gel universal combined pH/reference electrode.

DNA binding experiments

Water was purified using a Purelab Option R7 water purifier. MOPS (chemical name: 3-(*N*-morpholino)propanesulfonic acid, CAS [1132-61-2]), NaCl and EDTA (chemical name: ethylenediaminetetraacetic acid disodium salt dihydrate, CAS [6381-92-6]) were obtained from Fisher and used as supplied. Fish sperm DNA (Acros) was dissolved in buffer and dialysed (3.5 kDa MWCO) extensively against 2 l of buffer. The fish sperm DNA was found to be essentially protein free as $A_{260}/A_{280} = 2.05$. DNA concentrations were determined spectrophotometrically using $\varepsilon_{260nm} = 12800$ M(bp)$^{-1}$ cm^{-1} (the GC-content of vertebrates typically falls in the 38%–46% bracket[35] and variations in ε_{260nm} are expected to be rather limited within this range[36]).

All experiments were carried out in aqueous MOPS buffers (25 mM MOPS titrated to pH 7.0, 1 mM EDTA, and 50 mM NaCl) containing either 10 vol% DMSO (ITC) or a trace of acetone (UV-Vis) as co-solvents.

Isothermal titration calorimetry (ITC)

Calorimetric titrations were carried out at 25 °C on a high-precision VP-ITC microcalorimeter (MicroCal, LLC Northampton, MA).[37] The instrument was operated in high gain mode, applying a reference power of 10 μcal s^{-1} while stirring the sample cell contents at 307 or 416 rpm. A concentrated fish sperm DNA solution was dialysed (MWCO 3.5 kDa) extensively against buffer, diluted using the final dialyzate and made up to 10 vol% DMSO as required. Complex solutions were freshly prepared from a stock solution in DMSO as required, again using the final fish sperm DNA dialyzate. All solutions were degassed immediately before use.

Typically, complex dilution experiments were set up so that 20 μL of a 1 mM **ReL^1** solution was added to a known volume (approximately 1.9 ml including overflow) of buffer in the sample cell every 10 min up to a total of 13 injections. Following the first set of 13 injections, the cell contents were mixed with the combined excess cell solution and the solution that was expelled during the titration. The resulting solution was replaced into the calorimeter sample cell and a further 13 injections of 20 ml of **ReL^1** solution were made, resulting in

2 partially overlapping partial titrations.[32a] Titrations involving fish sperm DNA were carried out in several stages if needed using a 1 mM **ReL^1** solution in the syringe and different oligonucleotide concentrations (in the range of 50–250 μM base pairs) to "challenge" our binding model. Injections were typically made once every 10–15 min. Raw data was concatenated if needed (using ConCat32) and treated as usual using Origin to generate both integrated heat effects per injection (dh) and molar heat effects per injection (ndh).

Experiments using the model free ITC approach involved 5 injections of a 1.0 mM **ReL^1** solution into a 2.0 mM(bp) fish sperm DNA solution up to a molar ratio (**ReL^1**/DNA base pairs) of 0.05 at 25 °C, as well as all the required reference injections. All solutions were prepared as described above; the instrument was operated in high gain mode, applying a reference power of 10 μcal s^{-1} while stirring the sample cell contents at 502 rpm.

Circular dichroism and UV visible titrations

Combined UV-Vis and CD titrations were performed using an Applied Photophysics Chirascan spectropolarimeter coupled to a Julabo AWC100 water bath acting as a stable heat sink. A stock solution of **ReL^1** was prepared by dissolving in a minimal volume of acetone and making up to a 1 mM solution using MOPS buffer. The **ReL^1** stock solution was diluted as required. Titrations were performed by adding aliquots of concentrated DNA solutions to approximately 2 ml of a 5 μM and a 13 μM solution of **ReL^1** at 25 °C. After every addition, UV-Vis and CD spectra were recorded between (at least) 300 nm and 425 nm. Absorbances at 352 nm (A_{352}) in 1.00 cm pathlength cells were read from these spectra and fit to a multiple independent (but identical) binding site type model using Origin, correcting for **ReL^1** dilution.

Crystallography

Crystal data and data collection and refinement parameters for *fac*-{$Re(CO)_3$(**L^1**)}(BF_4) are given in Table 1, selected bond lengths and angles in Table 2.

Data collection and processing

Diffraction data were collected on a Bruker KAPPA APEX 2 using graphite-monochromated Mo-Kα radiation (k = 0.71073 Å) at 100 K. Software package Apex 2 (v2.1) was used for the data integration, scaling and absorption correction.

Structure analysis and refinement

The structure was solved by direct methods using SHELXS-97 and was completed by iterative cycles of ΔF-syntheses and full-matrix least squares refinement. All non-H atoms were refined anisotropically and difference Fourier syntheses were employed in positioning idealised hydrogen atoms and were allowed to ride on their parent C-atoms. All refinements were against F^2 and used SHELX-97.[38]

Syntheses of the ligands and complexes

Synthesis of L^1. To a solution of sodium tris(acetoxy)-borohydride (0.69 g, 3.25 mmol) in 4 ml dichloroethane was added stepwise, dipicolylamine (0.50 g, 2.5 mmol) and pyrenecarboxaldehyde (0.58 g, 2.52 mmol). The reaction mixture was stirred under nitrogen for 5 h. The reaction mixture was neutralised with sodium hydrogen carbonate and extracted with ethyl acetate and evaporated. The residue was chromatographed on a silica column and eluted with dichloromethane–methanol (90 : 10). The primary fluorescent band (LW 365 nm) was collected. The product was obtained as a light yellow oil which ultimately solidifies when dry (yield 0.3 g, 30%). MS m/z 436 $\{M + Na\}^+$, 414 $\{M + H\}^+$; UV-Vis (MeOH)/nm λ (ε = 1 mol^{-1} cm^{-1}) 266 (30 670), 276 (31 200), 300 (5900), 314 (14 200), 328 (28 300), 345 (13 100); ^{1}H NMR (400 MHz, $CDCl_3$): δ_H 8.45 (2H, d, $^3J_{HH}$ = 5 Hz), 8.3 (1H, d, $^3J_{HH}$ = 9 Hz), 7.9–8.1 (8H, m), 7.55 (2H, m), 7.4 (2H, t, $^3J_{HH}$ = 8 Hz), 7.05 (2H, t, $^3J_{HH}$ = 1 Hz), 4.3 (2H, s, CH_2), 3.8 (4H, s, CH_2).

Synthesis of L^2. To a solution of sodium tris(acetoxy)-borohydride (0.69 g, 3.25 mmol) in 4 ml dichloroethane was added stepwise, dipicolylamine (0.50 g, 2.5 mmol) and quinoxalinecarboxaldehyde (0.40 g, 2.5 mmol). The reaction mixture was stirred under nitrogen for 5 h. The reaction mixture was neutralised with sodium hydrogen carbonate and extracted with ethyl acetate and evaporated to dryness. The residue was chromatographed on a silica column and eluted with dichloromethane–methanol (90 : 10). The primary fluorescent band (LW 365 nm) was collected. The product was obtained as a viscous brown oil (yield 0.49 g, 57%). MS m/z 342 $\{M + H\}^+$; UV-Vis (MeOH)/nm λ (ε = 1 mol^{-1} cm^{-1}) 263 (66 000), 320 (55 000); ^{1}H NMR (400 MHz, $CDCl_3$): δ_H 9.1 (1H, s), 8.5 (2H, m), 8.05 (2H, m), 7.7 (2H, t, $^3J_{HH}$ = 4 Hz), 7.55 (2H, m), 7.5 (2H, d, $^3J_{HH}$ = 8 Hz), 7.1 (2H, m), 4.1 (2H, s, CH_2), 3.9 (4H, s, CH_2).

Synthesis of *fac*-{$ReCl(CO)_3$(L^1)}. To a solution of **L^1** (0.11 g, 0.257 mmol) in 10 ml of toluene was added rhenium pentacarbonylchloride (0.10 g, 0.277 mmol). The reaction mixture was heated to 100 °C and stirred under nitrogen for 3 h. A pale yellow precipitate formed. The product was filtered, washed with diethyl ether, dried and isolated as a white solid (yield 0.12 g, 60%). HR ESI MS found m/z 684.129, calculated m/z 684.129 for $\{M - Cl\}^+$; UV-Vis (MeOH)/nm λ (ε = 1 mol^{-1} cm^{-1}) 267 (27 800), 277 (31 100), 300 (9900), 315 (14 500), 329 (25 400), 345 (29 700); IR ($CHCl_3$) ν/cm^{-1}: 2033, 1935, 1916 (C≡O); ^{1}H NMR (400 MHz, $CDCl_3$): δ_H 8.7 (1H, d, $^3J_{HH}$ = 8 Hz), 8.55 (2H, d, $^3J_{HH}$ = 5 Hz), 8.5 (1H, d, $^3J_{HH}$ = 8 Hz), 8.3 (2H, d, $^3J_{HH}$ = 8 Hz), 8.2 (2H, m), 8.1 (2H, m), 8.0 (1H, m), 7.85 (2H, d, $^3J_{HH}$ = 8 Hz), 7.65 (2H, m), 7.05 (2H, t, $^3J_{HH}$ = 6 Hz), 6.1 (2H, d, $\frac{1}{2}$ × ($2CH_2$), $^2J_{HH}$ = 16 Hz), 5.5 (2H, s, py), 4.65 (2H, d, $\frac{1}{2}$ × ($2CH_2$), $^2J_{HH}$ = 16 Hz).

Synthesis of *fac*-{$Re(CO)_3$(L^1)}(BF_4). To a solution of *fac*-{$ReCl(CO)_3$(**L^1**)} (0.05 g, 0.070 mmol) in 10 ml acetonitrile was added silver tetrafluoroborate (0.014 g, 0.070 mmol). The reaction mixture was protected from light, heated to 60 °C and stirred under nitrogen for 18 h. A precipitate of silver chloride formed which was removed by filtration. The solvents were removed *in vacuo*. The pale brown oil was dissolved in acetonitrile (5 ml) and a pale brown solid precipitated with the addition of diethyl ether (5 ml). The product was filtered,

washed and isolated as an off-white solid in quantitative yield. HR ESI MS found m/z 684.131, calculated m/z 684.129 for $\{M\}^+$; UV-Vis (MeOH)/nm λ (ε = 1 mol^{-1} cm^{-1}) 267 (24 500), 277 (28 800), 300 (9100), 315 (13 300), 329 (22 800), 345 (25 300); IR ($CHCl_3$) ν/cm^{-1}: 2033, 1936, 1918 (C≡O); ^{1}H NMR (400 MHz, $CDCl_3$): δ_H 8.6 (2H ,d, $^3J_{HH}$ = 5 Hz), 8.55 (1H, d, $^3J_{HH}$ = 9 Hz), 8.4 (1H, d, $^3J_{HH}$ = 8 Hz), 8.3 (2H, m), 8.2 (2H, d, $^3J_{HH}$ = 8 Hz), 8.1 (2H, m), 8.0 (1H, m), 7.7 (2H, m), 7.6 (2H, d, $^3J_{HH}$ = 8 Hz), 7.1 (2H, t), 5.45 (2H, s, CH_2), 5.05 (2H, d, $\frac{1}{2}\times$ ($2CH_2$), $^2J_{HH}$ = 16 Hz), 4.7 (2H, d, $\frac{1}{2}\times$ ($2CH_2$), $^2J_{HH}$ = 16 Hz).

Synthesis of *fac*-{ReCl(CO)$_3$(L^2)}. To a solution of L^2 (0.094 g, 0.276 mmol) in 10 ml toluene was added rhenium pentacarbonylchloride (0.1 g, 0.276 mmol). The reaction mixture was heated to 60 °C and stirred under nitrogen for 3 h. A yellow precipitate formed. The product was filtered, washed and dried with diethyl ether and isolated as a bright yellow solid (yield 0.17 g, 94%). HR ESI MS found m/z 612.104, calculated m/z 612.104 for $\{M - Cl\}^+$; UV-Vis (MeOH)/nm λ (ε = 1 mol^{-1} cm^{-1}) 266 (52 000), 317 (35 000); IR ($CHCl_3$) ν/cm^{-1}: 2032, 1934, 1921 (C≡O); ^{1}H NMR (400 MHz, $CDCl_3$): δ_H 9.0 (1H, s), 8.6 (2H, d, $^3J_{HH}$ = 6 Hz), 8.1 (1H, d, $^3J_{HH}$ = 8 Hz), 7.95 (1H, d, $^3J_{HH}$ = 15 Hz), 7.65–7.8 (4H, m), 7.15 (2H, d, $^3J_{HH}$ = 6 Hz), 7.1 (2H, d, $^3J_{HH}$ = 8 Hz), 6.35 (2H, broad s), 5.2 (4H, broad s, CH_2).

Synthesis of *fac*-{Re(CO)$_3$(L^2)}(BF_4). To a solution of *fac*-{ReCl(CO)$_3$(L^2)} (0.05 g, 0.077 mmol) in 10 ml of acetonitrile was added silver tetrafluoroborate (0.015 g, 0.077 mmol). The reaction mixture was protected from light, heated to 60 °C and stirred under nitrogen for 18 h. A precipitate of silver chloride formed which was removed by filtration. The solvents were removed *in vacuo*. The pale yellow oil was then dissolved in acetonitrile (5 ml) and a pale yellow solid precipitated with the addition of diethyl ether (5 ml). The product was filtered, washed and isolated as a pale yellow solid in quantitative yield. HR ESI MS found m/z 612.105, calculated m/z 612.104 for $\{M\}^+$; UV-Vis (MeOH)/nm λ (ε = 1 mol^{-1} cm^{-1}) 266 (57 900), 325 (31 000); IR ($CHCl_3$) ν/cm^{-1}: 2034, 1935, 1921 (C≡O); ^{1}H NMR (400 MHz, $CDCl_3$): δ_H 9.05 (1H, s), 8.8 (2H, d, $^3J_{HH}$ = 5 Hz), 8.1 (1H, m), 7.95 (1H, d, $^3J_{HH}$ = 2 Hz), 7.8–7.9 (4H, m), 7.45 (2H, d, $^3J_{HH}$ = 8 Hz), 7.3 (2H, m), 5.3 (2H, d, $\frac{1}{2}\times$ ($2CH_2$), $^2J_{HH}$ = 17 Hz), 5.25 (2H, s), 4.9 (2H, d, $\frac{1}{2}\times$ ($2CH_2$), $^2J_{HH}$ = 17 Hz).

Acknowledgements

The EPSRC are thanked for support (EP/E048390/1 and EP/D001641/1) together with the Universities of Sheffield, Huddersfield and Cardiff.

References

1 T. Storr, K. H. Thompson and C. Orvig, *Chem. Soc. Rev.*, 2006, **35**, 534.
2 S. Lui, *Chem. Soc. Rev.*, 2004, **33**, 445.
3 R. Alberto, K. Ortner, N. Wheatley, R. Schibli and P. A. Schubiger, *J. Am. Chem. Soc.*, 2001, **123**, 3135.
4 M. Wrighton and D. L. Morse, *J. Am. Chem. Soc.*, 1974, **96**, 998.
5 (*a*) L. Sacksteder, A. P. Zipp, E. A. Brown, J. Streich, J. N. Demas and B. A. DeGraff, *Inorg. Chem.*, 1990, **29**, 4335; (*b*) J. V. Caspar, B. P. Sullivan and T. J. Meyer, *Inorg. Chem.*, 1984, **23**, 2104; (*c*) A. P. Zipp, L. Sacksteder, J. Streich, A. Cook, J. N. Demas and B. A. DeGraff, *Inorg. Chem.*, 1993, **32**, 5629; (*d*) L. Sacksteder, M. Lee, J. N. Demas and B. A. DeGraff, *J. Am. Chem. Soc.*, 1993, **115**, 8230; (*e*) B. D. Rossenaar, D. J. Stufkens and A. Vlcek, Jr, *Inorg. Chem.*, 1996, **35**, 2902; (*f*) A. J. Lees, *Chem. Rev.*, 1987, **87**, 711; (*g*) C.-C. Ko, L.-X. Wu, K. M.-C. Wong, N. Zhu and V. W.-W. Yam, *Chem.–Eur. J.*, 2004, **10**, 766; (*h*) S. M. Fredericks, J. C. Luong and M. S. Wrighton, *J. Am. Chem. Soc.*, 1979, **101**, 7415; (*i*) J. N. Demas and B. A. DeGraff, *Anal. Chem.*, 1991, **63**, 829A.
6 A. J. Amoroso, M. P. Coogan, J. E. Dunne, V. Fernández-Moreira, J. Hess, A. J. Hayes, D. Lloyd, C. Millet, S. J. A. Pope and C. Williams, *Chem. Commun.*, 2007, 3066.
7 (*a*) J. S. Kim, O. J. Shon, J. A. Rim, S. K. Kim and J. Yoon, *J. Org. Chem.*, 2002, **67**, 2348; (*b*) T. Jin, *Chem. Commun.*, 1999, 2491.
8 A.-J. Tong, A. Yamauchi, T. Hayashita, Z.-Y. Zhang, B. D. Smith and N. Termae, *Anal. Chem.*, 2001, **73**, 1530.
9 K.-S. Foscaneanu and J. C. Scaiano, *Photochem. Photobiol. Sci.*, 2005, **4**, 817.
10 H. K. Cho, D. H. Lee and J.-I. Hong, *Chem. Commun.*, 2005, 1690.
11 D. Y. Sakaki and B. E. Padilla, *Chem. Commun.*, 1998, 1581.
12 (*a*) S. Leroy, T. Soujanya and F. Fages, *Tetrahedron Lett.*, 2001, **42**, 1665; (*b*) A. C. Benniston, A. Harriman, D. J. Lawrie, A. Mayeux, K. Rafferty and O. D. Russell, *Dalton Trans.*, 2003, 4762.
13 X. Guo, D. Zhang, T. Wang and D. Zhu, *Chem. Commun.*, 2003, 914.
14 B. Bodenant, F. Fages and M.-H. Delville, *J. Am. Chem. Soc.*, 1998, **120**, 7511.
15 J. Y. Lee, S. K. Kim, J. H. Jung and J. S. Kim, *J. Org. Chem.*, 2005, **70**, 1463.
16 A. Okamoto, T. Ichiba and I. Saito, *J. Am. Chem. Soc.*, 2004, **126**, 8364.
17 (*a*) A. F. Morales, G. Accorsi, N. Armaroli, F. Barigelletti, S. J. A. Pope and M. D. Ward, *Inorg. Chem.*, 2002, **41**, 6711; (*b*) A. Del Guerzo, S. Leroy, F. Fages and R. H. Schmehl, *Inorg. Chem.*, 2002, **41**, 359; (*c*) N. D. McClenaghan, F. Barigelletti, B. Maubert and S. Campagna, *Chem. Commun.*, 2002, 602; (*d*) D. S. Tyson and F. N. Castellano, *J. Phys. Chem. A*, 1999, **103**, 10955.
18 (*a*) S. Faulkner, M.-C. Carrie, S. J. A. Pope, J. Squire, A. Beeby and P. G. Sammes, *Dalton Trans.*, 2004, 1405; (*b*) S. J. A. Pope, *Polyhedron*, 2007, 4818.
19 (*a*) N. Agorastos, L. Borsig, A. Renard, P. Antoni, G. Viola, B. Spingler, P. Kurz and R. Alberto, *Chem.–Eur. J.*, 2007, **13**, 3842; (*b*) P. Haefliger, N. Agorastos, A. Renard, G. Giambonini-Brugnoli, C. Marty and R. Alberto, *Bioconjugate Chem.*, 2005, **16**, 582.
20 A. Rescifina, U. Chiacchio, A. Piperno and S. Sortino, *New J. Chem.*, 2006, **30**, 554.
21 (*a*) A. C. Benniston, A. Harriman, D. J. Lawrie and M. Mehrabi, *Eur. J. Org. Chem.*, 2005, 1384; (*b*) M. Hariharan, J. Joseph and D. Ramaiah, *J. Phys. Chem. B*, 2006, **110**, 24678.
22 (*a*) H. C. Becker and B. Nordén, *J. Am. Chem. Soc.*, 1999, **121**, 11947; (*b*) H. C. Becker and B. Nordén, *J. Am. Chem. Soc.*, 2000, **122**, 8344.
23 M. E. C. D. Real Oliveira, A. L. F. Baptista, P. J. G. Coutinho, E. M. S. Castanheira and G. Hungerford, *Photochem. Photobiol. Sci.*, 2004, **3**, 217.
24 (*a*) A. J. Boersma, B. L. Feringa and G. Roelfes, *Org. Lett.*, 2007, **9**, 3647; (*b*) G. Roelfes, *Mol. BioSyst.*, 2007, **3**, 126; (*c*) G. Roelfes, A. J. Boersma and B. L. Feringa, *Chem. Commun.*, 2006, **6**, 635; (*d*) G. Roelfes and B. L. Feringa, *Angew. Chem., Int. Ed.*, 2005, **44**, 3230.
25 Although L^1 has been reported we were unable to retrieve details of its synthesis: S. Bhattacharya and A. Gulyani, *Chem. Commun.*, 2003, 1158.
26 (*a*) L. Wei, J. W. Babich, W. Ouellette and J. Zubieta, *Inorg. Chem.*, 2006, **45**, 3057; (*b*) S. R. Banerjee, P. Schaffer, J. W. Babich, J. F. Valliant and J. Zubieta, *Dalton Trans.*, 2005, 3886; (*c*) S. R. Banjeree, J. W. Babich and J. Zubieta, *Inorg. Chim. Acta*, 2006, **359**, 1608.
27 M. Frei, F. Marotti and F. Diedrich, *Chem. Commun.*, 2004, 1362.

28 C. Yao, H.-B. Kraatz and R. P. Steer, *Photochem. Photobiol. Sci.*, 2005, **4**, 191.
29 K. Bijma, J. B. F. N. Engberts, M. J. Blandamer, P. M. Cullis, P. M. Last, K. D. Irlam and L. G. Soldi, *J. Chem. Soc., Faraday Trans.*, 1997, 1579.
30 C. Wang, S. D. Wettig, M. Foldvari and R. E. Verrall, *Langmuir*, 2007, **23**, 8995.
31 J. B. Chaires, *Methods Enzymol.*, 2001, **340**, 3.
32 (*a*) N. J. Buurma and I. Haq, *J. Mol. Biol.*, 2008, **381**, 607; (*b*) J. R. Kiser, R. W. Monk, R. L. Smalls and J. T. Petty, *Biochemistry*, 2005, **44**, 16988; (*c*) S. Mazur, F. A. Tanious, D. Y. Ding, A. Kumar, D. W. Boykin, I. J. Simpson, S. Neidle and W. D. Wilson, *J. Mol. Biol.*, 2000, **300**, 321; (*d*) S. Mallena, M. P. H. Lee, C. Bailly, S. Neidle, A. Kumar, D. W. Boykin and W. D. Wilson, *J. Am. Chem. Soc.*, 2004, **126**, 13659.
33 I. Haq, T. C. Jenkins, B. Z. Chowdhry, J. Ren and J. B. Chaires, *Methods Enzymol.*, 2000, **323**, 373.
34 J. B. Chaires, *Arch. Biochem. Biophys.*, 2006, **453**, 26.
35 A. E. Vinogradov, *Cytometry*, 1998, **31**, 100.
36 J. Ren and J. B. Chaires, *Biochemistry*, 1999, **38**, 16067.
37 T. Wiseman, S. Williston, J. F. Brandts and L. N. Lin, *Anal. Biochem.*, 1989, **179**, 131.
38 G. M. Sheldrick, *SHELXL-97, Program for refinement of crystal structures*, University of Göttingen, Germany, 1997.